ACS SENSORS

Article

Cite This: ACS Sens. 2019, 4, 69−75

pubs.acs.org/acssensors

Electrochemical Biosensor Based on Surface Imprinting for Zika Virus Detection in Serum

Chompoonuch Tancharoen,[†] Wannisa Sukjee,[†] Chutima Thepparit,[‡] Thitigun Jaimipuk,[‡] Prasert Auewarakul,[§] Arunee Thitithanyanont,[∥] and Chak Sangma*[,†,⊥]

[†]Department of Chemistry, Faculty of Science, Kasetsart University, Bangkok 10900, Thailand

[‡]Institute of Molecular Biosciences, Mahidol University, Bangkok, Nakhon Pathom 73170, Thailand

[§]Department of Microbiology, Faculty of Medicine Siriraj Hospital, Mahidol University, Bangkok 10700, Thailand

[∥]Department of Microbiology, Faculty of Science, Mahidol University, Bangkok 10400, Thailand

[⊥]Center for Advanced Studies in Nanotechnology for Chemical, Food and Agricultural Industries, Kasetsart University Institute for Advanced Studies, Kasetsart University, Bangkok 10900, Thailand

S *Supporting Information*

ABSTRACT: Zika virus (ZIKV) is a flavivirus that was first identified in 1947. Initially, the virus was of little concern for health authorities given there were very few casualties among those suffering an infection. As such, only limited studies were performed on ZIKV. Recently, the viral infection has been linked to microcephaly in infants, which has prompted a dramatic increase in scientific interest in ZIKV research, including methods to allow for rapid virus identification. In this work we report the development of a new type of ZIKV electrochemical biosensor based on surface imprinted polymers and graphene oxide composites. The biosensor was used to detect ZIKV by measuring changes in the electrical signal with changing virus concentrations in buffer and serum using standard electrochemical techniques. The detection limit of our method is similar to the detection limit of the real-time quantitative reverse transcription PCR method.

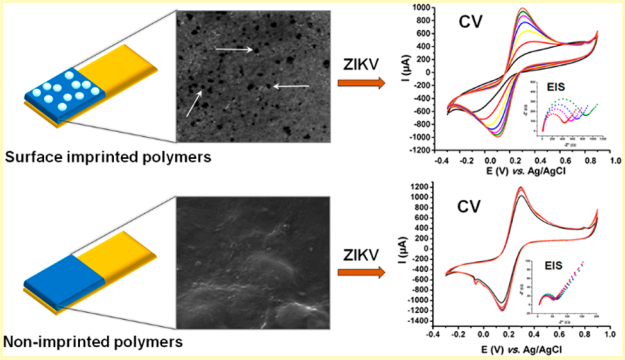

KEYWORDS: *Zika virus, surface imprinted polymers, biosensor, electrochemical sensor, cyclic voltammetry*

Zika virus (ZIKV) is a member of the *Flaviviridae* virus family that was first identified in monkeys in 1947, followed by humans in 1952.[1] ZIKV has spread to more than 50 countries worldwide, including almost all countries in Central/South America, the Caribbean, and South-East Asia,[2−4] with an estimated 3−4 million cases of infection.[5,6] ZIKV disease is caused by the transmission of this virus to people, primarily via the bite of daytime-active *Aedes* (*Ae.*) mosquitoes, such as *Ae. aegypti* and *Ae. albopictus*.[7] Infected individuals typically develop a mild fever, red eyes, a skin rash, conjunctivitis, muscle and joint pain, malaise, or headache. These symptoms normally start within 2−12 days after being bitten by a carrier mosquito and last for 4−7 days without any serious effects.[6] However, the major concern regarding this disease comes from the increased risk of microcephaly in babies born to women infected with ZIKV during pregnancy.[8−10] A rapid and simple method of detection of this infection could increase help in early screening and efficient monitoring of this disease.[11,12] Currently, the gold standard for ZIKV detection is based on real-time RT-PCR, and a rapid detection method has yet to be made available.[13,14] Several other approaches are being developed, including graphene-enabled biosensors, loop-mediated isothermal amplification, biomolecular sensors, CRISPR-based tools, and electrochemical sensors.[15−19]

Electrochemical sensors have many features that are suitable for ZIKV detection. This type of sensor offers rapid response, high sensitivity, and ease of use. There are a variety of materials that can be used for generating the virus-sensing layer, including antibodies, aptamers, or functionalized materials that exhibit target recognition in a manner that results in a change in electronic properties upon binding of the virus. Composites of functionalized materials, such as surface imprinted polymers (SIPs) and conductive nanoparticles, can achieve this objective. SIPs exhibit recognition via the self-assembly of monomers around the target template before polymerization and cross-linking reactions. After template removal, the SIP surfaces contain cavities that can recognize that template. SIPs from some virus species have been reported, and some of these SIPs have been successfully

Received: August 22, 2018
Accepted: December 31, 2018
Published: December 31, 2018

DOI: 10.1021/acssensors.8b00885
ACS Sens. 2019, 4, 69−75

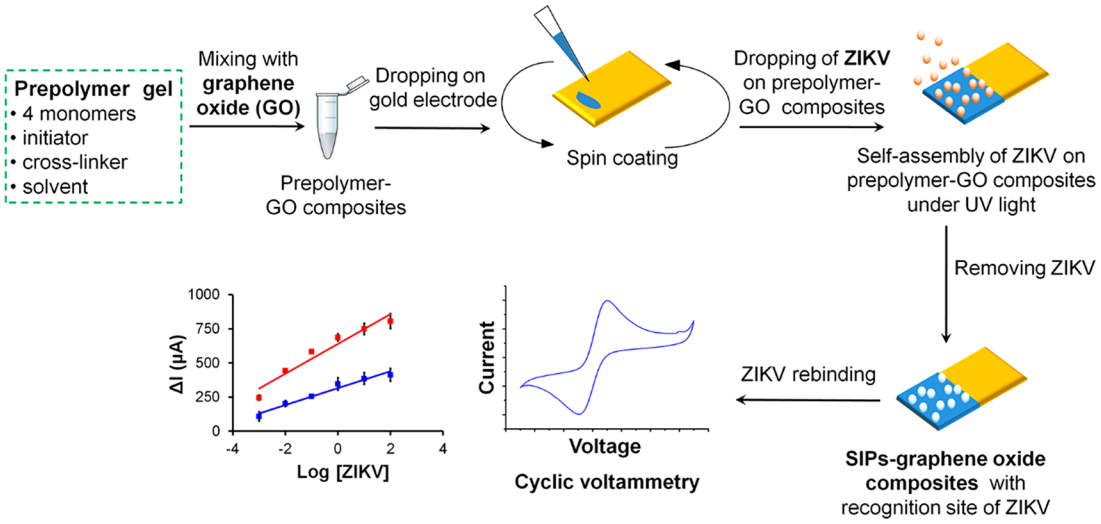

Figure 1. Scheme depicting SIPs-graphene oxide composites preparation on a gold surface for making the ZIKV biosensor. When Zika virus was added to the composites, some particles would have chances to be on the copolymers sites. At that time, the copolymers were partially polymerized and the self-assembly process by some prepolymer around the virus could occur. After the polymerization process had finished, the virus was removed and the recognition sites became cavities.

utilized as biosensors.[20−23] However, typical SIPs have very high electrical resistance and are not suitable for use in the formation of an electrochemically sensitive layer. Hence, by adding nanocarbon materials into these SIPs, electrochemical biosensors can be generated.[24−27] In this work, we constructed an electrochemical biosensor for ZIKV detection based on nanocarbon composites to detect ZIKV in both buffers and serum samples.

EXPERIMENTAL SECTION

ZIKV Propagation. The ZIKV particles required for biosensor fabrication by surface imprinting technique were propagated in a cell line. The ZIKV strain SV0127-14 (Zika virus/*H. sapiens*-tc/THA/2014/SV0127-14; GenBank, KU681081) was isolated from blood collected from patients in Thailand in 2014. This ZIKV strain was obtained by intrathoracic inoculation into *Toxorhynchites splendens* mosquitoes, followed by inoculation and propagation in C6/36 cells, a cell line derived from *Ae. albopictus* larvae. C6/36 cells were maintained in minimum essential medium (MEM; Gibco, Life Technologies, NY, USA) with 10% fetal bovine serum (FBS; Gibco, Life Technologies) and 1× non-essential amino acids (Gibco, Life Technologies) at 32 °C. For viral propagation, C6/36 cells were infected with the virus in the presence of growth medium lacking FBS for 1 h. The infected cells were then added into the complete medium and grown further until cytopathic effects were observed. Virus particles in the medium were collected by centrifugation at 1,500 rpm for 5 min. The viral titer, i.e., ZIKV concentration, was determined by a plaque assay.

Plaque Assay. Plaque assays are used for counting virus particles. Not all virus particles are counted, only the number of infectious viruses which is called a plaque forming unit (PFU). Vero cells maintained in MEM supplemented with 5% FBS and 1× penicillin−streptomycin (Gibco, Life Technologies) were preseeded in 12-well tissue-culture plates (4×10^6 cells/plate) 1 day prior to infection. Viruses were serially diluted in serum-free MEM prior to infecting the pregrown Vero cell monolayers for 1 h at 37 °C in a 5% CO_2 incubator with rocking every 15 min. The infected cells were then overlaid with MEM supplemented with 1.2% Avicel RC-591 (FMC BioPolymer, PA, USA) and 2% FBS. At day 7 postinfection, the cells were fixed with 4% formalin/phosphate-buffered saline (PBS) and stained with 1% crystal violet to visualize plaque formation. The viral titer was calculated in terms of PFU/mL.

Generation of RNA Standard for Real-Time qRT-PCR. The RNA standard had to be purified from the ZIKV stock before it could be used to obtain the concentration in terms of RNA copies by the real-time quantitative revere transcription PCR (qRT-PCR) method. Here, an in vitro transcribed RNA of the ZIKV prM-E gene was used as an RNA standard for quantitation of the ZIKV RNA transcript. Zika viral RNA was extracted from ZIKV (SV0127-14) culture supernatant using TRIzol-LS Reagent (Ambion, TX, USA) and used as a template for cDNA synthesis using ImProm-II reverse transcriptase (Promega, WI, USA) according to the manufacturer's protocols for construction of the ZIKV prM-E DNA plasmid. The ZIKV prM-E fragment, which was approximately 2 kb in size, was amplified from cDNA using Platinum Taq high-fidelity polymerase (Invitrogen, CA, USA) with 10 pmol of specific ZIKV prM-E primers. The forward primer contained the T7 promotor sequence for in vitro RNA transcription. The PCR conditions consisted of an initial denaturation at 94 °C for 2 min, followed by 35 cycles of denaturation at 94 °C for 2 min, primer annealing at 55 °C for 30 s, and extension at 68 °C for 2 min. Then, the PCR product was visualized on 1% agarose gel and purified by the GenepHlow Gel/PCR Kit (Geneaid, New Taipei City, Taiwan). The purified ZIKV prM-E DNA fragment was ligated to the pGEM-T Easy vector (Promega) at 16 °C overnight, and the resulting plasmid was used to transform *Escherichia coli* (*E. coli*) Top10 competent cells. Recombination was verified by digestion with the *Sac*I-HF restriction enzyme (New England BioLabs Inc., MA, USA) and nucleotide sequencing. A 5 μg amount of the ZIKV prM-E DNA plasmid was linearized by the *Hind*III-HF restriction enzyme (New England BioLabs) and purified using the GenepHlow Gel/PCR Kit. In vitro transcription was performed using T7 RNA polymerase (New England BioLabs). The RNA transcribed *in vitro* was treated with RQ1 *Dnase* (Promega) and purified using the RNA Clean-Up Kit (Geneaid). The concentration of the RNA standard was determined by a Nanodrop 1000 spectrophotometer (ThermoFisher Scientific, MA, USA). The RNA copy number (molecules/μL) was calculated as follows: The concentration of RNA (g/μL)/[length of RNA (nucleotides) × 340 (molecular weight of RNA in g/mol)] × 6.022 × 10^{23} (Avogadro's number; molecular weight in grams).

Real-Time qRT-PCR. Real-time qRT-PCR is widely considered to be one of the most reliable virus assay methods. We have chosen this method to determine the ZIKV stock concentration and to act as a comparative method to our electrochemical method based on SIPs. The RNA extracted from the ZIKV stock with a known titer was amplified for comparative RNA copy number quantitation by one-

DOI: 10.1021/acssensors.8b00885
ACS Sens. 2019, 4, 69−75

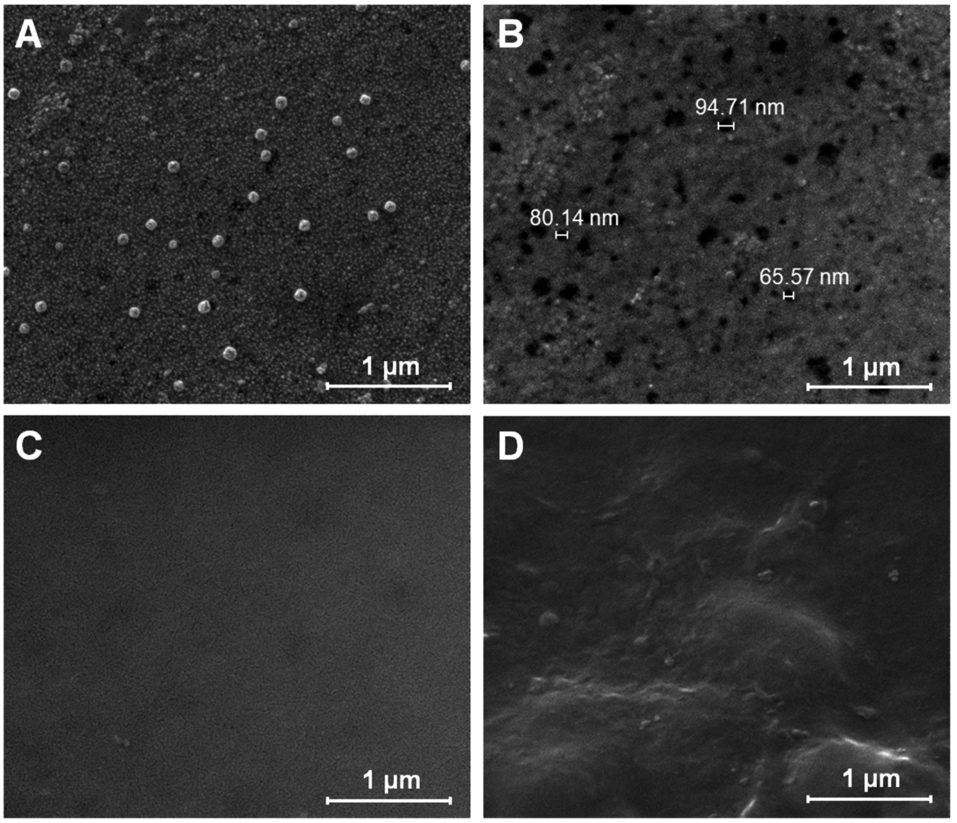

Figure 2. Surface characteristics of SIPs and NIPs were investigated using SEM. ZIKV particles (A) with 60−100 nm diameters we found to be associated with the cavities on the MIP surfaces after removal of the ZIKV template, the layer has approximately 8×10^6 cavities per square milliliter. (B). The NIP surfaces exhibited smooth areas both before (C) and after washing (D) with water.

step real-time qRT-PCR using KAPA PROBE FAST universal one-step qRT-PCR (Kapa Biosystems, Inc., MA, USA) in an Eppendorf Mastercycler RealPlex machine (Eppendorf, Inc., NY, USA). The probe and primers were specific to the Asian ZIKV E protein-encoding sequences according to the published "Bonn E" assay.[28] The nucleotide sequences of the primers and probe were as follows: forward primer, AGYCGYTGYCCAACACAAG; reverse primer, CACCARRC TCCCYTTGCCA; and probe, 5′FAM-CCTMCCTY-GAYAAGCARTCAGACACYCAA-3′BHQ1. Amplification was carried out in the reaction mixtures containing 1 × KAPA PROBE FAST qPCR master mix, 0.2 μM each primer, 0.2 μM fluorogenic probe, and RNase-free water to a final volume of 20 μL. The cycling conditions were as follows: reverse transcription at 42 °C for 10 min and initial activation of PCR at 95 °C for 5 min, followed by 40 cycles of two steps of cycling PCR, a denaturation step at 95 °C for 3 s, and an annealing and extension step at 60 °C for 20 s. The CT values of the samples of interest were calculated as the number of RNA molecules according to the standard curve generated by the plot of log concentration versus CT values of the serially diluted standard RNAs (10^1−10^8 molecules). In this work, the obtained RNA copy number from the ZIKV sample was 5,028 copies/PFU.

Surface Imprinted Polymers−Graphene Oxide Composites and Electrode Preparation. The sensing layer of the electrode was made from polymer and GO composites though ZIKV template imprinting. The SIP composite biosensor was prepared in multiple steps following the scheme depicted in Figure 1. First, the optimized prepolymer gel was prepared using four monomers; 20 mg of acrylamide (AAM; Merck, NJ, USA), 12 μL of methacrylic acid (MAA; Merck), 12 μL of methyl methacrylate (MMA; Merck), and 6.7 μL of *N*-vinylpyrrolidone (NVP; Merck) were mixed with 1.5 mg of free radical initiator (azobis(isobutyronitrile) (AIBN); Sigma-Aldrich, MO, USA) and 47 mg of cross-linker (*N*,*N*′-(1,2-dihydroxyethylene)bis(acrylamide) (DHEBA); Tokyo Chemical Industry, Tokyo, Japan) in 300 μL of dimethyl sulfoxide (DMSO; RCI Labscan, Bangkok, Thailand). The mixture was prepolymerized at 70 °C to reach the gel point. After reaching the gel point, the prepolymer was mixed with graphene oxide (Supporting Information Figure S1) dispersed in water (0.15 mg/mL) at a 2:3 ratio; the percentage in the imprinted layer was 60% (v/v) or 9% (w/v). Then, 10 μL of the prepolymer−graphene oxide mixture was coated on a 1 × 1 cm^2 gold electrode before spinning at 1,000 rpm for 10 s to remove excess prepolymer. In the final step, 5 μL of the ZIKV sample was dispersed on the composite film and exposed to UV light for 3 h before keeping in an oven at 65 °C for 15 h to allow polymerization to occur. The SIP composites were obtained after removing the ZIKV template from the composite surface by washing in 10% acetic acid (30 min) and deionized water at 50 °C (30 min). The nonimprinted polymers (NIPs) were prepared as described above but without the ZIKV template. The 1 × 1 cm^2 gold electrode was used to conduct measurements in PBS.

A small biosensor used to conduct experiments in serum was prepared on a 3.4 × 1.0 cm^2 screen-printed gold electrode (SPE) having gold as working and counter electrodes and a silver reference electrode (DRP-220BT, Dropsens, Asturias, Spain) as shown in Figure 5 (inset). The sensitive layer was coated on the working SPE (4 mm diameter). The SPE biosensor was produced following the procedure described above, but only 0.8 μL of the prepolymer−GO composites and 1 μL of ZIKV were used for imprinting. All biosensors were fabricated in a laminar flow cabinet (BSL-2).

Electrochemical Impedance Spectroscopy and Cyclic Voltammetry. Two electrochemical techniques, electrochemical impedance spectrscopy (EIS) and cyclic voltammetry (CV), were conducted in the experiment. EIS was used to validate that SIP composites can recognize ZIKV. This has been achieved by the stepwise comparison between the charge transfer resistance of bare electrode, NIP composites, and SIP composites in the presence of ZIKV. While CV was used to measure the current change with ZIKV and other background concentrations. Both CV and EIS experiments

DOI: 10.1021/acssensors.8b00885
ACS Sens. 2019, 4, 69−75

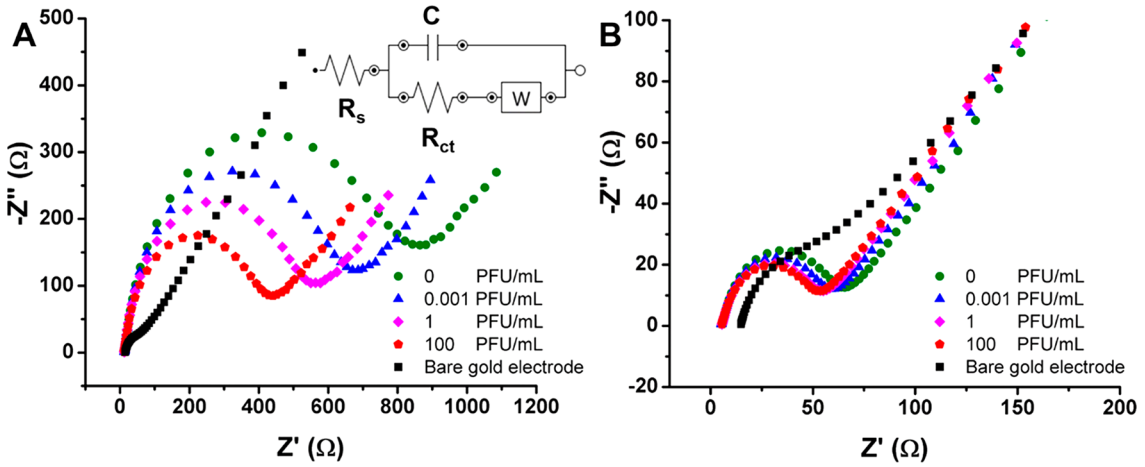

Figure 3. ZIKV recognition by the SIPs was demonstrated by EIS. R_{ct} value (related to Z'') of the SIP composite electrode decreased with virus concentration (A). No significant changes were observed from the experiment using the NIP electrode (B). An equivalent circuit for the Nyquist plot was used to calculate R_{ct} at different concentrations of ZIKV (inset).

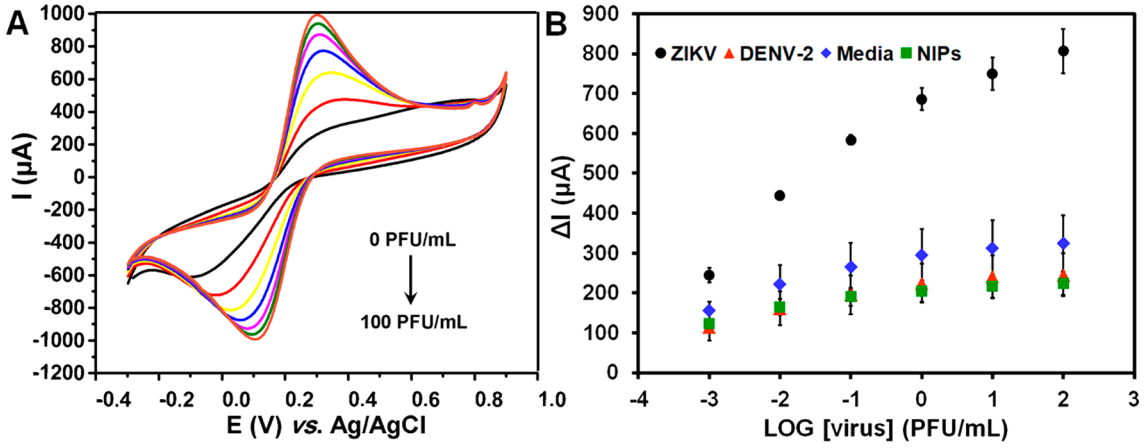

Figure 4. Cyclic voltammogram of different ZIKV concentrations in 0.01 M PBS obtained using a ZIKV SIP sensitive layer (A). The plot of current changes as a linear function of log virus concentration on the NIP and SIP electrode together with the results from the other control experiments using DENV-2 and media (B) (experiments carried out in triplicate).

were conducted with AutoLab PGSTAT302N (Metrohm Siam, Bangkok, Thailand). ZIKV samples were prepared by diluting the stock to the desired concentrations (0−100 PFU/mL) in 0.01 M PBS and 1 or 10% serum (from the Department of Microbiology, Faculty of Science, Mahidol University) containing 5 mM $K_4Fe(CN)_6$/$K_3Fe(CN)_6$ (ratio 1:1) as a redox couple. For ZIKV measurement in PBS, the 1 × 1 cm^2 gold working electrode was used for the CV and EIS scans with Ag/AgCl and platinum as the reference and counter electrodes, respectively. The experiments were carried out in 0.01 M PBS containing a redox couple with 0.001, 0.01, 0.1, 1, 10, and 100 PFU/mL ZIKV at 20 mL total volume. Dengue virus type 2 (DENV-2) and virus cultivation media (from Institute of Molecular Biosciences, Mahidol University) were selected for cross-selectivity and background interference measurements. The data were collected from CV scans between −0.3 and +0.9 V at a scan rate of 50 mV/s.

The EIS experiment was conducted at 0.3 V with a 0.01−10,000 Hz frequency scan. Impedance data were presented as the Nyquist plots ($-Z''$ versus Z') from samples having 0, 0.001, 1, and 100 PFU/mL ZIKV in 20 mL of PBS using the SIP and NIP composite sensors. The charge transfer resistance (R_{ct}) was calculated by NOVA 1.11 software using the RCRW equivalent circuit (Figure 3A inset).

For ZIKV determination in 1 and 10% serum, the experiments were carried out using the SIP biosensor on SPE. The ZIKV samples were prepared in 1 and 10% serum containing a redox couple for CV measurement at 80 μL total volume. The CV experiment was carried out between −0.4 and +0.7 V at 50 mV/s scan rate. The gold plate electrode could be used 12 times, and the SPE could be used 7 times.

Scanning Electron Microscopy. A Quanta 450 FEI instrument for scanning electron microscopy (SEM) was used to examine the morphology of the ZIKV SIP and NIP surfaces using secondary electrons generated at 20 keV. Both ZIKV SIP and NIP samples were prepared on gold surfaces as described above.

RESULTS AND DISCUSSION

SEM Images of ZIKV SIPs and NIPs on Electrode Surfaces. The SEM images in Figure 2 show how the imprinting process changed the composite surface, generating active sites in the presence of ZIKV templates. Before the removal of the ZIKV template, ZIKV was distributed on the surface (Figure 3A), in contrast to the smooth surface of the corresponding NIP composites (Figure 2C). However, after washing out the templates, the pores with diameter equal to the averaged ZIKV diameter (80 nm) could be seen on the SIP composites (Figure 2B), in contrast to the surface of the corresponding NIP composites, which were not imprinted with ZIKV (Figure 2D).

ZIKV Recognition by SIPs. The effect of virus imprinting on ZIKV recognition by the SIP composites was validated first by EIS and then by CV. The EIS experiment was used to

DOI: 10.1021/acssensors.8b00885
ACS Sens. 2019, 4, 69−75

follow the R_{ct} of the electrode surfaces before and after coating with SIP and NIP composites, followed by successively adding ZIKV at different concentrations to both systems. By calculating the impedance value (Z) after each frequency scan, the Nyquist plot, which is a plot between the $-Z''$ versus Z' components of Z, could be obtained. In the case of the bare electrode, the Nyquist plot was linear, indicating that there was no contribution from R_{ct} to Z (the black dotted lines in Figure 3A). After coating with polymer composites, the Nyquist plots showed semicircular patterns for both SIPs and NIPs, where the magnitude of R_{ct} (based on the circuit analog shown in the Figure 3A inset) was represented by the diameter of the semicircle. It was found that the R_{ct} of the ZIKV SIP composites electrode reduced with the change in ZIKV concentration (Figure 3A), whereas the corresponding value for the NIP electrode remained unchanged (Figure 3B).

This ability to differentiate the signals from different ZIKV concentrations was used to confirm successful imprinting. The decrease in impedance with increasing ZIKV concentration in the solution indicated that the absorption of ZIKV on the SIP biosensor increased the conductivity. Therefore, we decided to use CV to measure the current gained as a function of ZIKV concentration as the assay protocol; the obtained Nyquist plot was a semicircle with a decreasing trend, followed by signal saturation at high concentrations.

It was found that the CV results were consistent with the results from the EIS experiments. The ZIKV selectivity of the SIP biosensor was validated by comparing the signals from the SIP and NIP composite biosensors using ZIKV, dengue virus, and virus cultivation media. Upon increasing the ZIKV concentration, only the SIP biosensor produced a high CV signal change. The NIP biosensor remained almost unchanged (Figure 4B). The highest current gain at each concentration was obtained for the sample in PBS (Figure 4A), with linearity observed at up to six log-scale concentrations from 10^{-3} to 10^{2} PFU/mL. The limit of detection (LOD) for ZIKV in PBS was 2×10^{-4} PFU/mL. Since we tried to demonstrate a new method of Zika virus detection, we needed the result from a standard method such as real-time qRT-PCR for comparison. According to real-time qRT-PCR assay (in section Real-Time qRT-PCR), the ZIKV used in this experiment contained 5,000 RNA copies/PFU, implying that the LOD in PBS corresponded to 1 RNA copy/mL. However, the results from two other experiments in the presence of dengue virus and media exhibited lower detection limits of 2×10^{-2} PFU/mL (100 times higher than the value in buffer solution).

Measurement of ZIKV in Serum by the SPE Biosensor. Real-world detection of ZIKV in patient derived samples requires an ability to analyze blood serum.[29,30] Therefore, tests to see whether our biosensor could be applied under such conditions were conducted. A 1×1 cm^2 gold electrode was replaced by an SPE biosensor that used only 80 μL due to the small volume of serum available. Background interference at high serum concentrations was observed upon comparing the signal to that observed in PBS (Figure S2). Therefore, measurement in serum requires sample dilutions to at least 10% of the serum concentration (Figure 5). The results showed that the LOD of ZIKV in 1 and 10% serum increased to 2×10^{-3} and 5×10^{-2} PFU/mL (or 10 and 250 RNA copies/mL), respectively. These LODs were calculated from the signal-to-noise ratio ($S/N = 3$) at 95% confidence interval. These LODs could correspond to an ability to detect ZIKV in samples from an infected patient with 0.2 and 0.5 PFU/mL ZIKV (or 10 and 50 RNA copies/mL), respectively, in a nondiluted serum sample.

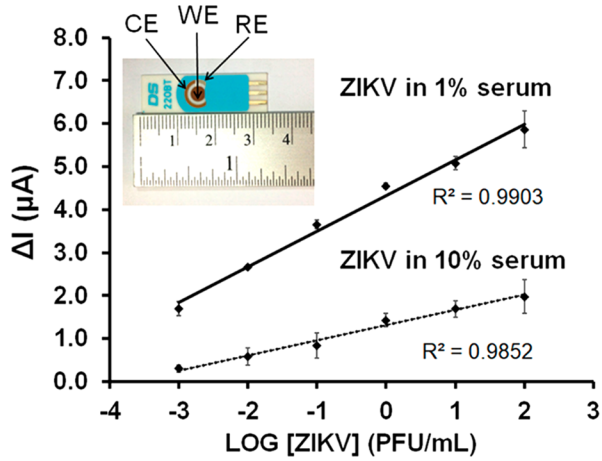

Figure 5. Linear plots of current versus ZIKV concentrations gains from ZIKV SIP composites coated on SPE in 1 and 10% blood serum. The SPE has gold (4 mm diameters) as a working electrode (WE) and counter electrode (CE), silver as a reference electrode (RE) (inset).

CONCLUSIONS

We have demonstrated a method for the rapid detection of ZIKV using an electrochemical biosensor prepared from SIP composites. The biosensor was functional in both PBS and blood serum environments. In PBS, the biosensor could be used to detect ZIKV at concentrations as low as 2×10^{-4} PFU/mL (1 RNA copy/mL). The LOD was found to be 2×10^{-2} PFU/mL in the presence of dengue virus and media. In serum, dilution was required to reduce the background signal. The LOD increased to 2×10^{-3} and 5×10^{-2} PFU/mL (10–250 RNA copies/mL) in 10 and 1% serum samples, respectively. We estimated the number of virus particles by manually counting from the SEM image available and found that the Zika virus stock had approximately 5.1×10^{11} particles/mL (Figure S3 in the Supporting Information). In PFU the same sample had 1.7×10^{7} PFU/mL, so 1 PFU contained approximately 3×10^{4} Zika virus particles. According to this, the detection limit of the sensor had increased from 6 particles/mL in buffer solution to 60, 600, and 600 particles/mL in 1% serum, media, and dengue virus environments, respectively. Neglecting the buffer LOD and taking into account the effect of sample dilution, the lowest detection limit in real samples should be 6000 ($\sim 10^4$) particles (or $\sim 10^{-3}$ PFU) per mL. This LOD value is sufficient for ZIKV detection in real-world applications.[31,32] It should be noted that we did not need to filter or centrifuge the serum sample. This was because proteins or other substances in these samples could not be removed without affecting the virus concentration. Nonetheless, the signals in these environments exhibited the same range of linearity as those in PBS. Further experiments on additional patient derived samples are required to confirm the utility of the results in real-world use.

ASSOCIATED CONTENT

Supporting Information

The Supporting Information is available free of charge on the ACS Publications website at DOI: 10.1021/acssensors.8b00885.

DOI: 10.1021/acssensors.8b00885
ACS Sens. 2019, 4, 69–75

SEM image of graphene oxide, signals from blank buffer and serums, and SEM image of Zika virus particles (PDF)

AUTHOR INFORMATION

Corresponding Author

*E-mail: fscicsm@ku.ac.th.

ORCID

Chak Sangma: 0000-0002-2627-8073

Notes

The authors declare no competing financial interest.

ACKNOWLEDGMENTS

This work was supported by the Thailand Research Fund (TRF), the Royal Golden Jubilee Ph.D. Program (RGJ; Grant No. PHD/0170/2556). We thank Kasetsart University Research and Development Institute (KURDI) and the National Research University Project of Thailand (NRU). We also thank the Armed Forces Research Institute of Medical Sciences (AFRIMS) and the Department of Disease Control, Ministry of Public Health, Thailand, for providing the Zika viral isolates used in this study. Additionally, we thank the Department of Biochemistry, Faculty of Science, Kasetsart University, for providing the BSL-2 workspace. Finally, we thank Prof. Matthew Paul Gleeson for his help in editing and revising the manuscript.

REFERENCES

(1) Dick, G. W. A.; Kitchen, S. F.; Haddow, A. J. Zika Virus (I). Isolations and serological specificity. *Trans. R. Soc. Trop. Med. Hyg.* **1952**, *46*, 509−520.

(2) Gyawali, N.; Bradbury, R. S.; Taylor-Robinson, A. W. The global spread of Zika virus: is public and media concern justified in regions currently unaffected? *Infect. Dis. Poverty* **2016**, *5*, 37 DOI: 10.1186/s40249-016-0132-y.

(3) Vorou, R. Zika virus, vectors, reservoirs, amplifying hosts, and their potential to spread worldwide: what we know and what we should investigate urgently. *Int. J. Infect. Dis.* **2016**, *48*, 85−90.

(4) Lim, S. K.; Lim, J. K.; Yoon, I. K. An Update on Zika Virus in Asia. *Infect. Chemother.* **2017**, *49*, 91−100.

(5) Samarasekera, U.; Triunfol, M. Concern over Zika virus grips the world. *Lancet* **2016**, *387*, 521−524.

(6) *Zika situation report, Zika and Potential Complications*;World Health Organization, Feb. 12, 2016.

(7) Local Mosquito-Borne Transmission of Zika Virus-Miami-Dade and Broward Counties, FL, June−August 2016. *Morbidity and Mortality Weekly Report (MMWR)*; Centers for Disease Control and Prevention, 2016.

(8) Brasil, P.; Pereira, J. P. J.; Moreira, M. E.; Ribeiro Nogueira, R. M.; Damasceno, L.; Wakimoto, M.; Rabello, R. S.; Valderramos, S. G.; Halai, U.-A.; Salles, T. S.; Zin, A. A.; Horovitz, D.; Daltro, P.; Boechat, M.; Raja Gabaglia, C.; Carvalho de Sequeira, P.; Pilotto, J. H.; Medialdea-Carrera, R.; Cotrim da Cunha, D.; Abreu de Carvalho, L. M.; Pone, M.; Machado Siqueira, A.; Calvet, G. A.; Rodrigues Baião, A. E.; Neves, E. S.; Nassar de Carvalho, P. R.; Hasue, R. H.; Marschik, P. B.; Einspieler, C.; Janzen, C.; Cherry, J. D.; Bispo de Filippis, A. M.; Nielsen-Saines, K. Zika Virus Infection in Pregnant Women in Rio de Janeiro. *N. Engl. J. Med.* **2016**, *375*, 2321−2334.

(9) Cauchemez, S.; Besnard, M.; Bompard, P.; Dub, T.; Guillemette-Artur, P.; Eyrolle-Guignot, D.; Salje, H.; Van Kerkhove, M. D.; Abadie, V.; Garel, C.; Fontanet, A.; Mallet, H.-P. Association between Zika virus and microcephaly in French Polynesia, 2013−15: a retrospective study. *Lancet* **2016**, *387*, 2125−2132.

(10) Johansson, M. A.; Mier-y-Teran-Romero, L.; Reefhuis, J.; Gilboa, S. M.; Hills, S. L. Zika and the Risk of Microcephaly. *N. Engl. J. Med.* **2016**, *375*, 1−4.

(11) Lee, K. H.; Zeng, H. Aptamer-Based ELISA Assay for Highly Specific and Sensitive Detection of Zika NS1 Protein. *Anal. Chem.* **2017**, *89*, 12743−12748.

(12) Lamb, L. E.; Bartolone, S. N.; Tree, M. O.; Conway, M. J.; Rossignol, J.; Smith, C. P.; Chancellor, M. B. Rapid Detection of Zika Virus in Urine Samples and Infected Mosquitos by Reverse Transcription-Loop-Mediated Isothermal Amplification. *Sci. Rep.* **2018**, *8*, 3803.

(13) Faye, O.; Faye, O.; Diallo, D.; Diallo, M.; Weidmann, M.; Sall, A. A. Quantitative real-time PCR detection of Zika virus and evaluation with field-caught mosquitoes. *Virol. J.* **2013**, *10*, 311.

(14) Xu, M. Y.; Liu, S. Q.; Deng, C. L.; Zhang, Q. Y.; Zhang, B. Detection of Zika virus by SYBR green one-step real-time RT-PCR. *J. Virol. Methods* **2016**, *236*, 93−97.

(15) Acharya, D.; Bastola, P.; Le, L.; Paul, A. M.; Fernandez, E.; Diamond, M. S.; Miao, W.; Bai, F. An ultrasensitive electrogenerated chemiluminescence-based immunoassay for specific detection of Zika virus. *Sci. Rep.* **2016**, *6*, 32227.

(16) Pardee, K.; Green, A. A.; Takahashi, M. K.; Braff, D.; Lambert, G.; Lee, J. W.; Ferrante, T.; Ma, D.; Donghia, N.; Fan, M.; Daringer, N. M.; Bosch, I.; Dudley, D. M.; O'Connor, D. H.; Gehrke, L.; Collins, J. J. Rapid, Low-Cost Detection of Zika Virus Using Programmable Biomolecular Components. *Cell* **2016**, *165*, 1255−1266.

(17) Song, J.; Mauk, M. G.; Hackett, B. A.; Cherry, S.; Bau, H. H.; Liu, C. Instrument-Free Point-of-Care Molecular Detection of Zika Virus. *Anal. Chem.* **2016**, *88*, 7289−7294.

(18) Tian, B.; Qiu, Z.; Ma, J.; Zardan Gomez de la Torre, T.; Johansson, C.; Svedlindh, P.; Stromberg, M. Attomolar Zika virus oligonucleotide detection based on loop-mediated isothermal amplification and AC susceptometry. *Biosens. Bioelectron.* **2016**, *86*, 420−425.

(19) Afsahi, S.; Lerner, M. B.; Goldstein, J. M.; Lee, J.; Tang, X.; Bagarozzi, D. A.; Pan, D.; Locascio, L.; Walker, A.; Barron, F.; Goldsmith, B. R. Novel graphene-based biosensor for early detection of Zika virus infection. *Biosens. Bioelectron.* **2018**, *100*, 85−88.

(20) Wangchareansak, T.; Thitithanyanont, A.; Chuakheaw, D.; Gleeson, M. P.; Lieberzeit, P. A.; Sangma, C. Influenza A virus molecularly imprinted polymers and their application in virus subtype classification. *J. Mater. Chem. B* **2013**, *1*, 2190−2197.

(21) Altintas, Z.; Gittens, M.; Guerreiro, A.; Thompson, K.-A.; Walker, J.; Piletsky, S.; Tothill, I. E. Detection of Waterborne Viruses Using High Affinity Molecularly Imprinted Polymers. *Anal. Chem.* **2015**, *87*, 6801−6807.

(22) Liang, C.; Wang, H.; He, K.; Chen, C.; Chen, X.; Gong, H.; Cai, C. A virus-MIPs fluorescent sensor based on FRET for highly sensitive detection of JEV. *Talanta* **2016**, *160*, 360−366.

(23) Sukjee, W.; Thitithanyanont, A.; Wiboon-ut, S.; Lieberzeit, P. A.; Paul Gleeson, M.; Navakul, K.; Sangma, C. An influenza A virus agglutination test using antibody-like polymers. *J. Biomater. Sci., Polym. Ed.* **2017**, *28*, 1786−1795.

(24) Ma, Y.; Shen, X.-L.; Zeng, Q.; Wang, H.-S.; Wang, L.-S. A multi-walled carbon nanotubes based molecularly imprinted polymers electrochemical sensor for the sensitive determination of HIV-p24. *Talanta* **2017**, *164*, 121−127.

(25) Navakul, K.; Warakulwit, C.; Yenchitsomanus, P.; Panya, A.; Lieberzeit, P. A.; Sangma, C. A novel method for dengue virus detection and antibody screening using a graphene-polymer based electrochemical biosensor. *Nanomedicine* **2017**, *13*, 549−557.

(26) Sukjee, W.; Tancharoen, C.; Yenchitsomanus, P.; Gleeson, M. P.; Sangma, C. Small-Molecule Dengue Virus Co-imprinting and Its Application as an Electrochemical Sensor. *ChemistryOpen* **2017**, *6*, 340−344.

(27) Ghanbari, K.; Roushani, M. A nanohybrid probe based on double recognition of an aptamer MIP grafted onto a MWCNTs-Chit

DOI: 10.1021/acssensors.8b00885
ACS Sens. 2019, 4, 69−75

nanocomposite for sensing hepatitis C virus core antigen. *Sens. Actuators, B* **2018**, *258*, 1066−1071.
(28) Corman, V. M.; Rasche, A.; Baronti, C.; Aldabbagh, S.; Cadar, D.; Reusken, C. B.; Pas, S. D.; Goorhuis, A.; Schinkel, J.; Molenkamp, R.; Kummerer, B. M.; Bleicker, T.; Brunink, S.; Eschbach-Bludau, M.; Eis-Hubinger, A. M.; Koopmans, M. P.; Schmidt-Chanasit, J.; Grobusch, M. P.; de Lamballerie, X.; Drosten, C.; Drexler, J. F. Assay optimization for molecular detection of Zika virus. *Bull. World Health Organ* **2016**, *94*, 880−892.
(29) St. George, K.; Sohi, I. S.; Dufort, E. M.; Dean, A. B.; White, J. L.; Limberger, R.; Sommer, J. N.; Ostrowski, S.; Wong, S. J.; Backenson, P. B.; Kuhles, D.; Blog, D.; Taylor, J.; Hutton, B.; Zucker, H. A. Zika Virus Testing Considerations: Lessons Learned from the First 80 Real-Time Reverse Transcription-PCR-Positive Cases Diagnosed in New York State. *J. Clin. Microbiol.* **2017**, *55*, 535−544.
(30) Murray, K. O.; Gorchakov, R.; Carlson, A. R.; Berry, R.; Lai, L.; Natrajan, M.; Garcia, M. N.; Correa, A.; Patel, S. M.; Aagaard, K.; Mulligan, M. J. Prolonged Detection of Zika Virus in Vaginal Secretions and Whole Blood. *Emerging Infect. Dis.* **2017**, *23*, 99−101.
(31) Lustig, Y.; Mendelson, E.; Paran, N.; Melamed, S.; Schwartz, E. Detection of Zika virus RNA in whole blood of imported Zika virus disease cases up to 2 months after symptom onset, Israel, December 2015 to April 2016. *Euro Surveill.* **2016**, *21*, No. 30269, DOI: 10.2807/1560-7917.ES.2016.21.26.30269.
(32) Musso, D.; Rouault, E.; Teissier, A.; Lanteri, M. C.; Zisou, K.; Broult, J.; Grange, E.; Nhan, T. X.; Aubry, M. Molecular detection of Zika virus in blood and RNA load determination during the French Polynesian outbreak. *J. Med. Virol.* **2017**, *89*, 1505−1510.

DOI: 10.1021/acssensors.8b00885
ACS Sens. 2019, 4, 69−75